Parametrization of GROMOS Force Field for Oligosaccharides and Assessment of Efficiency of Molecular Dynamics Simulations*

KARL-HEINZ OTT[†] and BERND MEYER[‡]

Complex Carbohydrate Research Center and Department of Biochemistry and Chemistry, The University of Georgia, 220 Riverbend Road, Athens, Georgia 30602

Received 6 January 1995; accepted 30 August 1995

ABSTRACT

Molecular dynamics (MD) simulations of α-D-maltose (maltose) *in vacuo* and with explicit inclusion of water were performed using the GROMOS force field that was modified to include a potential energy term for the exo-anomeric effect. Different simulation temperatures, the influence of the size of the water box, and carbohydrate-specific force field parameter values were evaluated with respect to sampling efficiency and average conformations. First, maltose was surrounded by 500 water molecules and simulated for 750 ps. Furthermore, three 500-ps MD simulations *in vacuo* were run to identify the effect of solvation on the location of the preferred conformation and on the flexibility of the molecule. Inclusion of water leads to a change of the preferred conformation from $\varphi/\psi^1 \approx -20°/-17°$ *in vacuo* to $-40°/-31°$ in aqueous solution. The explicit incorporation of water molecules into the simulation gave rise to only short-lived hydrogen bond interactions. In particular, a hydrogen bond found *in vacuo* from OH3 of the reducing glucose to O2′ of the nonreducing glucose was rarely present when water was included in the simulation. *In vacuo* the conformational freedom of the glycosidic linkage and the hydroxymethyl and hydroxyl groups were strongly reduced due to intramolecular hydrogen bonds. Two 200-ps MD runs with inclusion of 137 water molecules at temperatures of 350 and 400 K showed the expected increase of the transitions between the

*This article includes Supplementary Material available from the authors upon request or via the Internet at ftp.wiley.com/public/journals/jcc/suppmat/17/1068 or http://www.wiley.com/jcc

[†]Author to whom all correspondence should be addressed at American Cyanamid Co., P.O. Box 400, Princeton, NJ 08543-0400. E-mail: ottk@pt.cyanamid.com

[‡]Present address: Institut für Organische Chemie, M. L. King Platz 6, 20146 Hamburg, Germany.

CCC 0192-8651 / 96 / 081068-17

rotamers of the hydroxymethyl groups. An equilibrium for the conformation of the glycosidic linkage was only reached when raising the temperature parameter of the MD simulation further to 600 K. However, at this temperature inversions of the pyranose ring were already observed within a 1-ns MD simulation. Parametrization of GROMOS to include the exo-anomeric effect proved to be necessary because the previously published force field has no provisions to account for the exo-anomeric effect, as revealed by two MD simulations in water and *in vacuo* that indicated a significant population at positive φ angles. Using dimethoxymethane as a model for the *O*-glycosidic linkage, the empirical potential function for the rotation about the C1—O1 bond was adjusted to represent the potential calculated by STO 6-31G* *ab initio* calculations. MD simulations using the adjusted force field revealed a reduced population with positive φ values. A separate parametrization of the potential for the reducing hydroxyl group of saccharides resulted in a better description of the conformation, as well as increased stability of the integration algorithm. Finally, the existing GROMOS force field was supplemented by an additional *gauche* potential. Its effect on the conformation of the hydroxymethyl groups was evaluated by a 500-ps MD simulation in water. © 1996 by John Wiley & Sons, Inc.

Introduction

Molecular dynamics (MD) simulations with empirically derived potential energy functions (force fields) provide a comprehensive description of conformations, dynamics, and molecular interactions in solution[1-3] and also aid in the interpretation of experimental data.[4-7] Preferred conformations of carbohydrates have been investigated experimentally and by energy calculations *in vacuo*.[8] However, effects of solvation of oligosaccharides have only recently been under close investigation.[9-19] Generalized force fields have been adapted for the use with carbohydrates[20-22] to calculate their conformations in free solution[18,23-26] and it is intended to further develop these tools for calculations of carbohydrates in complexes with, or bound to, other molecules. Some disagreement between experimental data and time averaged calculated observables has been reported.[18,19,27,28] In particular, the electrostatic energy terms for those force fields appear to be still under development and the effect of hydration on the conformations and flexibility of solvated carbohydrates remains unclear.[19,29-31]

Molecular dynamics simulation of cyclodextrin using the GROMOS[32] force field[24] described carbohydrate solvent interactions and hydrogen bonding patterns in good agreement with crystallographic determined structures.[11,14,24,25] This force field has also been widely applied to calculate molecular dynamics of proteins,[33] lipids,[34] and DNA,[35] making GROMOS valuable for the calculation of conjugates or complexes of different molecular classes, although specialized force fields might be more accurate in the description of a single class of molecules. It has been shown that the *exo-anomeric* effect has a strong impact on the orientation and the conformational equilibrium of the glycosidic linkage.[36] Our initial investigations using the previously published GROMOS force field revealed that the orientation of the glycosidic linkage that is expected to be stabilized by the exo-anomeric effect has similar energy to the inverted conformation that is not stabilized by this stereo electronic effect.

Our first aim was to establish an empirical potential energy function that accounts for the stereo electronic effects of the glycosidic linkage, and that also is appropriate for the description of the interaction of carbohydrates with solvent, proteins, and lipids. The first part of this article describes the determination and implementation of additional energy terms to account for the exo-anomeric effect in the GROMOS force field. A careful evaluation and addition of potential energy terms has been aimed to retain consistency within the parameters of the force field. This consideration is of crucial importance[7] and prohibits the combination of different parametrizations from various force fields. MD simulations of maltose *in vacuo* and in water have been run both with and without the force field terms for the exo-anomeric effect, and the results are compared in order to characterize the force field parametrization.

Our second aim was to examine the efficiency of MD simulations using the modified GROMOS force field to generate a representative sampling of

the conformational space. The incorporation of water and different settings of simulation parameters, i.e., temperature and cutoff radii for nonbonded interactions, were analyzed in this respect. In a second study,[37] we present very long MD simulations that start from different conformations and reveal lifetimes and equilibrium conformations of maltose in solution. Those results agree very well with experimental NMR and optical rotation data for maltose in aqueous solution.

Methods

Atoms of the nonreducing glycosyl residue, residue 2, are indicated by a prime ('). The glycosidic linkage dihedral angles φ and ψ were calculated from the atomic coordinates of the C3, C4, O1', C1', and O5' atoms (φ_C, ψ_C) and converted into the values for φ = H1'—C1'—O1'—C4 (or H1—C1—O1—HO1) and ψ = C1'—O1'—C4—H4 by subtracting 120°. The hydroxymethyl orientations are described by the ω angles that are measured as O5—C5—C6—O6 for ω_1 and O5'—C5'—C6'—O6' for ω_2. They are described by two letters that refer the orientation toward O5 and C4, using *g* for *gauche* and *t* for *trans* orientations, e.g., *gt* has $\omega = 60°$.

All MD calculations used the program package GROMOS[32] adapted to FORTRAN 77 standard and compiled with double precision (64 bit) word length for floating point variables. Programs based on the GROMOS subroutine library were written to perform the systematic search for calculating energy surfaces and for additional data analysis. Most visual and statistical data analysis was accomplished by home written program modules for the PV ~ wave[38] graphical software package. Molecular structures were displayed with SYBYL.[39] The setup and analysis of the simulations was facilitated by a user interface to all these programs that was based on csh-scripts[40] and the awk programming language.[40]

FORCE FIELD PARAMETRIZATION

Parameters to account for the exo-anomeric effect within GROMOS were determined from the difference between the GROMOS' potential energy as a function of dihedral angles for dimethoxymethane and methoxymethanol and corresponding energy values from *ab initio* calculations.[41-43] Coordinates for dimethoxymethane and methoxymethanol were generated using standard bond lengths and bond angles.[24] One dihedral angle (τ) was set to 60° and 180° to model the α and β configuration of the anomeric carbon, respectively. The second dihedral angle (φ) was varied in 10° steps between 0° and 350°. To find the lowest energy for a conformation with given dihedral angle values, bond lengths and angles were adjusted by energy minimization (EM) steps using steepest descent and/or conjugate gradient minimization algorithms until convergence to 10^{-5} kJ mol^{-1} nm^{-1}. Both dihedral angles were kept on their preset position by applying dihedral restraint potentials with force constants of 5000 and 10,000 kJ mol^{-1} rad^{-1} for τ and φ, respectively.

Bond lengths were set to average values found by X-ray analysis of pyranoses.[44] Since all simulations were performed by applying the SHAKE[45] algorithm to bonds, no corrections or adjustment of force constants were necessary. The bond angle potential energy parameters for the glycosidic linkage and the reducing hydroxy group were adjusted by choosing appropriate values for the bond angle at the energy minimum. Their force constants were taken from the GROMOS parameter set.[24] The potential of the exo-anomeric effect was determined by fitting[46,47] a third-order Fourier series of cosine functions to the difference between the energies calculated with the empirical force field and energies calculated by *ab initio* methods. Parameters of this numerical adaptation were incorporated into GROMOS as additional dihedral angle potentials. The whole cycle was repeated twice.

The incorporation of the new parameters into the existing GROMOS force field that uses the united atom model could be achieved most practically by defining two new atom types, one for C1 and one for O1, and adding the related parameters to the interaction function parameter tables. Residue topologies were defined for each residue and each linkage separately (e.g., glucose with O2, O3, O4, and O6 as an open end). These residue topology building blocks were defined for most biologically relevant monosaccharides. A modified version (probmt) of the program progmt[32] was written to generate branched topologies for oligosaccharides and glycopeptides.[§]

[§]For structures with more than three branches (two branches if ions are present), a modified version of the GROMOS subroutine "CONAT" is also necessary.

MD SIMULATIONS

For the MD simulations in water, the start conformation was centered in a rectangular box with a minimum distance of 0.25 nm to the bounds for runs w, w35, w40, and w60, and a minimum distance of 0.4 nm for runs wb1 and wb2. The SPC water model was used.[48] Periodic boundary conditions with cutoff radii for nonbonded interactions of 0.8 nm for the former runs and 1.2 nm for the latter runs were applied. To avoid truncation artifacts, nonbonded interactions were calculated on the basis of an atom pair list that was updated every 25 integration cycles for the simulations in water. *In vacuo*, these interactions were calculated for all atom pairs. Electric neutrality of the pair interactions was assured by using the concept of charge groups, and a permeability constant of 1 was used for the Coulomb energy term. Initial velocities were assigned randomly according to a Maxwell distribution at 300 K. The solvent molecules were allowed to equilibrate during energy minimization and 50-ps MD simulation. During this time, the maltose atoms were kept close to their start positions by applying a harmonic pseudopotential with a force constant of 6250 kJ mol^{-1} nm^{-2}. The temperature was regulated by virtually coupling the atom's velocities to an external bath[49] with a relaxation constant of 0.1 ps. Solvent and solute atoms were scaled separately. For the MD runs at 300 and 350 K, the pressure of the system was kept at 1.013 bar by isotropically scaling the size of the computational box[49] with a relaxation constant of 0.5 ps. At higher temperatures (run w40 and w60), the volume of the box was constant (NTP ensemble). The width of the integration steps of the MD simulations was 2 fs. Bond lengths were constrained by applying the SHAKE[45] algorithm. Energy values, coordinates, and dihedral angles values were stored and analyzed in time steps of 100 fs.

Results

DERIVATION OF OLIGOSACCHARIDE FORCE FIELD PARAMETERS

Dimethoxymethane mimics the C5—O5—C1—O1—Cx unit in oligosaccharides, thereby representing a model for the acetal moiety of the glycosidic linkage for which high level *ab initio* data are available.[42] It is evident that the energy of dimethoxymethane as a function of the C1—O1 dihedral angle (Fig. 1) using the original GROMOS force field does not agree with data obtained from *ab initio* calculations. For both the α and the β anomers, the energy of the conformation representing an inverse exo-anomeric conformation ($\varphi = 60°$, $\varphi_C = 180°$) is about as low as the conformation that should be stabilized by the exo-anomeric effect ($\varphi = -60°$, $\varphi_C = 60°$). The energy values published by Wiberg and Murcko[42] and two additional energy values calculated for φ_C angles of 30° and 90° (ref. 43) were used to derive a force field term for GROMOS to account for the exo-anomeric effect.

For the C—O bonds length, GROMOS' standard equilibrium value of 1.435 Å was changed to 1.42, 1.4, and 1.39 Å for C1—O5 and C1—O1 in the α and β anomer,[42,44] respectively. The potentials that describe changes of the bond angles (τ) were incorporated into the GROMOS force field[24] as $V_{angle} = \Sigma^{1/2} k_\tau (\tau - \tau_0)^2$. In the original form, all atoms with tetrahedral configurations have an equilibrium value of $\tau_0 = 109.5°$. In the energy minimum ($\varphi_C = 67°$), this parameter leads to a bond angle of the glycosidic oxygen of $\tau = 111°$ for α and β anomers. However, the average bond angle of the glycosidic oxygen (C—O—C) found experimentally[44] and theoretically[42] is $\tau \approx 117°$ at the energy minimum. Changing the equilibrium value of the bond angle potential for the glycosidic oxygen atom to $\tau_0 = 113°$ results in a bond angle of $\approx 117°$ for the minimum energy conformation. The geometries of the other oxygen atoms showed good agreement with experimental data when using the default equilibrium values for the bond angle potential (Fig. 1C, D).

Adjustment of the dihedral angle potential for the α and β anomers resulted in the force constants k_i listed in Table I for the potential $V = \Sigma_i k_i [1 + \cos(i\varphi_C - \delta)]$, with $i = 1, 2, 3$. With this potential added, a calculation of the energy of the β anomer as a function of the C1—O1 dihedral angle yields a very good fit between the energy of the new empirical force field and that of the *ab initio* calculations as indicated by a standard deviation of $< 10^{-5}$ kJ mol^{-1} (cf. Fig. 1B). For the α anomer, the parameters that yielded the best description of the region of and between both minima at $\varphi_C \approx -60°$ and 60° were obtained using weight factors of 20 ($\varphi_C = +60°, -60°$), 10 ($-30°, 0°$), 3 (120°), 1 ($-90°$), and 0.5 ($180°, -120°$) for the fit. The *ab initio* data could be represented better with different weight factors. This parameter set was selected for several reasons that are detailed in the Discussion.

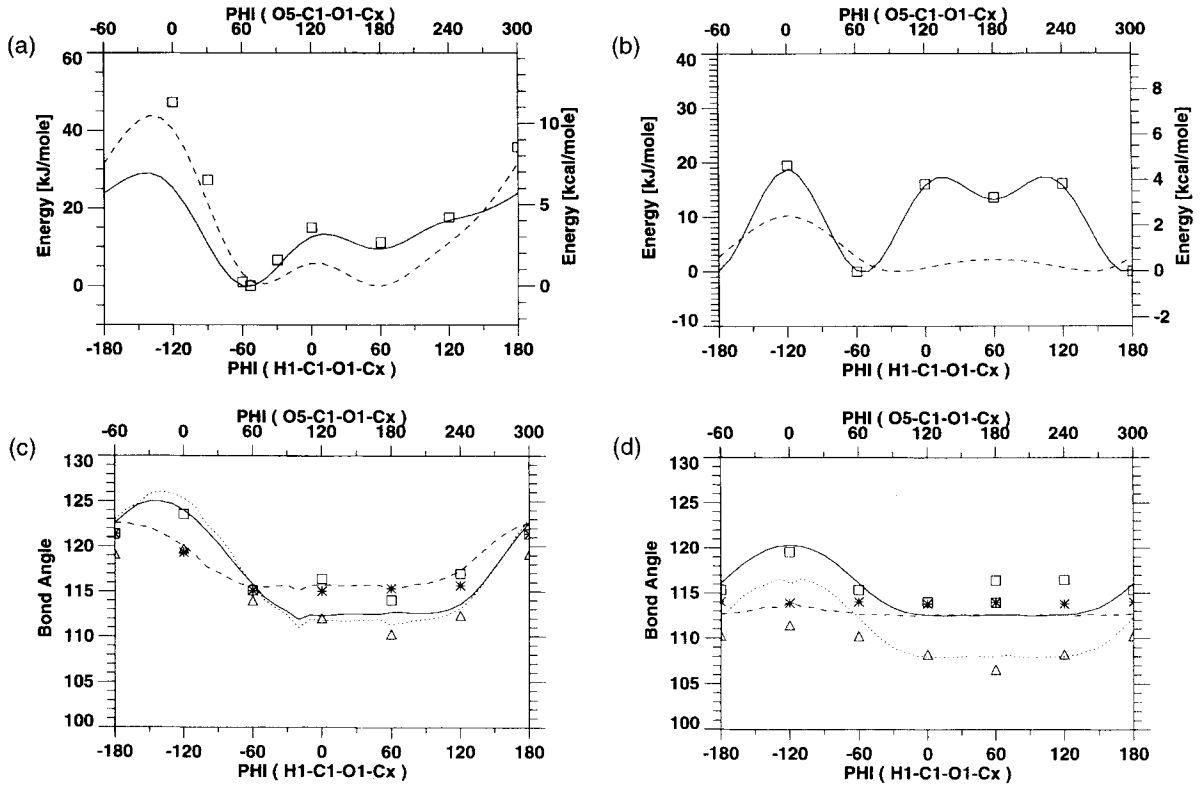

FIGURE 1. (A) Potential energy of dimethoxymethane in the α conformation ($\tau = 60°$) as a function of the C1 — O1 dihedral angle. The squares indicate the energy values obtained by *ab initio* STO 6-31G* calculations. (—) Potential energy surface calculated with the GROMOS force field with the exo-anomeric potential; (---) potential energy in the original force field.[25] (B) Same for the β anomer. (C) Bond angles in the new parametrized force field (with $\tau_{0(O1)} = 113°$, $\tau_{0(C,O5)} = 109.5°$) in dimethoxymethane in the α conformation. The symbols represent the values from the *ab initio* calculations, the lines with symbols are the corresponding values obtained after the force field modifications ((---), (●) (∠C1—O1—Cx; (···), (△) ∠O5—C1—O1; (---), (*) ∠C5—O5—C1. (D) Bond angle as in (C) but for the β conformation.

TABLE I.
Optimized Force Field Parameters.

	$n = 1$		$n = 2$		$n = 3$		τ_0
Multiplicity	k	δ	k	δ	k	δ	O1
COC alpha	9.64	180	1.85	180	−3.46	180	113.0
COC beta	6.74	180	−2.6	180	−5.44	180	113.0
HOC alpha	7.37	−75	7.55	−42	2.22	−30	113.5
HOC beta	15.14	180	−3.69	180	0.87	0	113.5

Parameters for the exo-anomeric potential (V_{ea}) to be used together with the parameters of ref. 24 for an *O*-glycosidic linkage in the α-D (COC alpha) and the β-D (COC beta) configuration and the α-D (HOC alpha) and the β-D (HOC beta) configuration in reducing saccharide residues. For the equations $V_{ea} = k_n[1 + \cos(n\varphi_c - \delta)]$ the force constants (k) and the shift value (δ) are listed for the function with multiplicity n. (*Note:* φ_c refers to the dihedral O5 — C1 — O1 — X, where X is the carbon or hydrogen atom that is attached to O1.) In the last column, the value for the equilibrium bond angle (τ_0) of the oxygen atom of the glycosidic linkage / the acetalic OH group is given (see text for details).

Using either the original GROMOS force field[24] or the modified force field for calculations of reducing sugars, we observed that the reducing O5—C1—O1—HO1 unit was often severely distorted.[14] For example, in the α configuration the minimum energy for a reducing sugar was found at $\varphi_C = 15°$, which is near the energy maximum predicted by an *ab initio* calculation[41] (Fig. 2). This[14] and related[‖] problems could be resolved by two changes to the force field. First, we removed the electrostatic interaction between the O5 and the HO1 atoms and set the C1—O1 bond length[44] to 1.395 Å. Second, the exo-anomeric potential for reducing sugars was derived by reference to the *ab initio* calculation of methoxymethanol[41] in an analogous manner as described above for dimethoxymethane. The optimized force field parameters are listed in Table I and the corresponding energy functions are depicted in Figure 2.

In practice, the atom types C1 and O1 are newly introduced into the GROMOS parameter set and are used for the anomeric carbon and the oxygen in *O*-glycosidic linkages, respectively. As before,[12] the atom type OS is used for the exo-cyclic oxygen in saccharides (e.g., O5); the atom type OA is used for all hydroxyl oxygens. Sugar CH units are characterized by atom type CS1; the deoxy sugar's and the hydroxymethyl's CH_2 groups are assigned to atom type CS2. The α and β anomers are not distinguished by atom types; specific parameters are assigned individually or via the residue topology building blocks.

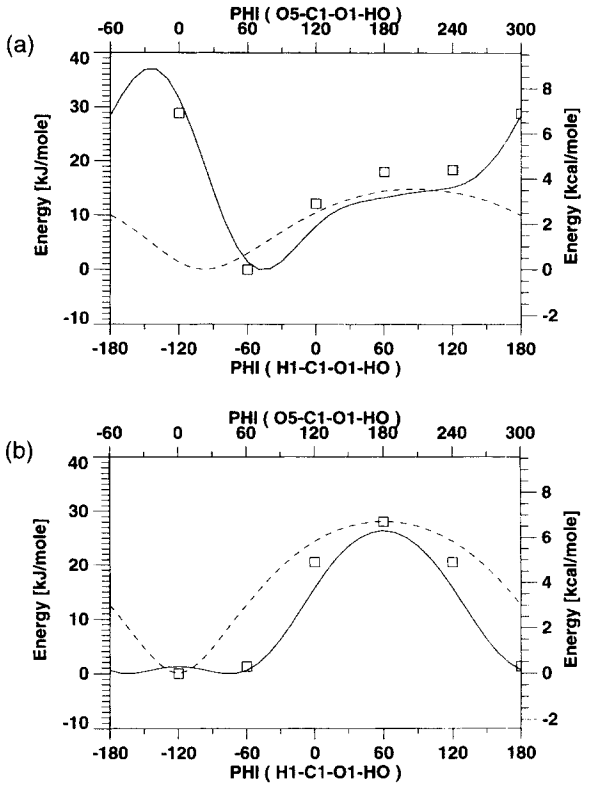

FIGURE 2. Same as Figure 1A, B for methoxymethanol in the (A) α-D and (B) β-D conformation.

MD SIMULATIONS OF MALTOSE

The MD simulations were carried out to investigate the influence of different simulation parameters and the solvent environment on the explored conformational space. The same start conformation that was arbitrarily selected from an MD simulation *in vacuo* (data not shown) with $\varphi/\psi = -11°/-20°$, $\omega_1 = -57°$, and $\omega_2 = 177°$ was used for all simulations except for run wb2 that was continued from run wb1. To evaluate the effect of the number of solvent molecules, the maltose was inserted in water boxes of different size. One box contained 499 water molecules (runs wb1 and wb2) and had edge lengths of about 2.5 nm each, which is equivalent to a concentration of the maltose solution of about 0.1 M. The other box contained 137 water molecules with edge lengths of about 1.7 nm each (runs w, w35, w40, w60), which is equivalent to a concentration of the maltose solution of about 0.4 M. The water boxes were first equilibrated by an energy minimization, and, subsequently, by 50-ps MD simulations with position restraints for the atoms of the maltose molecule. The following free MD simulations are in thermal equilibrium as indicated by stable total energy values. Energy statistics are available in the supplement.

In runs w35, w40, and w60, the temperature parameter of the simulations was increased to 350, 400, and 600 K, respectively, to evaluate whether an increase of the temperature could result in a more effective scanning of the conformational space without introducing artifacts. All other simulations were run at 300 K. For comparison, the results from MD calculations in water without the exo-anomeric potential (run w) and *in vacuo* with (run vb and vc) and without (run va) the exo-anomeric effect are also presented. An overview of the calculation is given in Table II. A summary of

[‖]Problems during the equilibration of model build systems are also related to the HO1—O5 interaction. Very small EM or MD step sizes had to be used to avoid too large displacements of the HO1 atom that could not be reset by the SHAKE algorithm.

TABLE II.
Overview and Statistics of MD Simulations.

run	wb1		wb2		w35		w40		w60		w		va		vb		vc	
φ(°)	−11		−52		−11		−11		−11		−11		−11		−11		−11	
ψ(°)	−20		−25		−20		−20		−20		−20		−22		−22		−22	
$\omega_1-\omega_2$	gg −tg		gg −gg		gy −tg		gg −tg		gg −tg		gg −tg		gg −tg		gg −tg		gg −tg	
Time (ps)	200		500		200		200		950		250		500		500		500	
Solvent #	499		499		137		137		137		137		0		0		0	
Temp. K	300		300		350		400		600		300		300		300		300	
rnr	ψ	φ	ψ	φ	ψ	φ	ψ	φ	ψ	φ	ψ	φ	ψ	φ	ψ	φ	ψ	φ
Avg (°)	−28	−41	−34	−46	−34	−44	−39	−48	−26	−53	−21	−22	−16	−18	−17	−20	−17	−21
SD (°)	17	18	14	14	18	19	18	17	37	33	24	27	13	18	13	13	12	13
Min (°)	−89	−98	−87	−93	−111	−97	−116	−110	−178	−179	−92	−100	−54	−74	−77	−103	−55	−78
Max (°)	27	16	40	12	31	15	37	15	180	180	48	66	27	55	33	33	35	22

For each run, the start conformations are indicated by the φ and ψ angles, and the ω angles of the reducing residue ($\omega 1$) and the nonreducing residue ($\omega 2$). Additionally, the length of free MD simulation time (ps), the number of solvent molecules (Solvent #), and the virtual temperature (Temp. K) are given. In the lower part of the table, resulting averages (Avg), standard deviations (SD), minimal (Min), and maximal (Max) values of φ and ψ angles from the MD simulation are listed.

the hydroxymethyl rotameric distribution is compiled in Table III.

MD Simulation with 499 Water Molecules, Run wb1

After releasing the constraints on the maltose that were applied to relax the water box, the glycosidic linkage shows a transition of its conformation to $\varphi/\psi \approx -25°/-16°$ where it stayed for the next 50 ps (Fig. 3). At about 100 ps, the conformation of the glycosidic linkage changed again slightly to adopt a stable conformation throughout the MD simulation of average $\varphi/\psi \approx -41°/-28°$ (Fig. 4). The hydroxymethyl group of the reducing end is in the *gg* form for most of the time with one short transition into the *gt* conformation. The nonreducing hydroxymethyl group undergoes six transitions, accessing all three staggered conformations with a population ratio of $gg : gt : tg = 40 : 50 : 10$ (Table III).

Most of the hydroxyl dihedral angles change rapidly between the staggered conformations. However, for the reducing hydroxyl group, only 14 transitions are observed between rotamers with a dihedral angle φ (O5—C1—O1—OH1) $\approx 75°$ that is populated to 80% and conformations that indicate a broad minimum around the inverse exo-anomeric conformation. A hydrogen bond is found between 60 and 82 ps where for 50% of the time a hydrogen bond is observed between OH2′ and O3. The opposite hydrogen bond between OH3 and O2′ occurs for 1.4 ps. These hydrogen bonds are correlated with dihedral angles of the glycosidic linkage of φ and ψ about 0°. Transient hydrogen bonds with lifetimes of less than 1 ps are observed between the hydroxymethyl groups.

MD Simulation with 499 Water Molecules and Additional Gauche Potential, Run wb2

Another 500-ps MD simulation of maltose in a water box containing 499 molecules was started with the conformation that was adopted at the end of the previous run, characterized by $\varphi/\psi = -52°/-25°$, $\omega_1 = -70°$, and $\omega_2 = -72°$. The MD simulation was run with an additional potential, $V = -6^*\cos(\varphi(\text{O—C—C—O}))$, (gauche potential) to more correctly reflect the energetics of a O—C—C—O fragment, the so-called gauche effect.[52] Thereby, the gauche orientation of vicinal oxygen atoms is stabilized by 4.5 kJ mol^{-1} relative to the trans orientation. This potential is an estimate that was derived from an analysis of the

TABLE III.
Summary of Hydroxymethyl Rotameric Distribution.

Run	Rot	ω(1) Pop	ω(1) %Pop	ω(1) Avg	ω(1) SD	ω(2) Pop	ω(2) %Pop	ω(2) Avg	ω(2) SD
wb1	*gt*	46	2	51	19	1060	53	66	15
	tg	0	0			180	9	163	17
	gg	1954	98	293	12	760	38	294	13
wb2	*gt*	1118	22	54	15	2750	55	53	16
	tg	0	0			222	4	163	14
	gg	3882	78	305	13	2028	41	305	14
w	*gt*	175	7	67	20	1711	68	67	17
	tg	82	3	159	18	507	20	161	18
	gg	2243	90	293	14	282	11	296	13
w35	*gt*	1609	80	67	18	41	2	65	20
	tg	382	19	154	17	3	0	233	3
	gg	9	0	301	30	1956	98	295	14
w40	*gt*	678	34	69	20	989	49	64	18
	tg	361	18	160	18	126	6	161	24
	gg	961	48	293	15	885	44	295	16
w60	*gt*	3059	32	67	24	3808	40	64	23
	tg	3059	32	165	23	2303	24	166	24
	gg	3382	36	292	19	3389	36	293	20
va	*gt*	0	0			1885	38	69	16
	tg	0	0			1779	36	175	14
	gg	5000	100	297	13	1336	27	291	14
vb	*gt*	999	20	62	15	787	16	70	16
	tg	647	13	165	14	3783	76	172	14
	gg	3354	67	297	13	430	9	291	14
vc	*gt*	0	0			1101	22	69	15
	tg	0	0			3894	78	173	14
	gg	5000	100	298	13	5	0	278	25

Statistical data of the hydroxymethyl population distribution given as absolute population (Pop) using one conformation every 100 fs for all MD simulations. The relative populations (%Pop) of the three rotameric states, *gt*, *gg*, and *tg*, their average ω angles, and corresponding standard deviation (SD) are also listed for the ω angle of the reducing [ω(1)] and the nonreducing [ω(2)] residue.

energy difference of glucose *in vacuo* in different conformations.

The conformation of the glycosidic linkage during the simulation is characterized by average φ/ψ dihedral angles of $\approx -46°/-34°$ with standard deviations of 14°/14° (Figs. 4 and 5). At about 100 ps, a small change can be observed in the φ/ψ trajectories. The averages of the φ/ψ angles in the first 100 ps are $-40°/-32°$, whereas during the last 400 ps this dihedral angle pair changed its average values to $-50°/-36°$. At $\approx$ 320-ps simulation time, positive dihedral angle values are observed for the glycosidic linkage.

The reducing hydroxymethyl group has six transitions between the *gt* and the *gg* conformations during the MD simulation. Conformations with a *tg* conformation are not observed for this hydroxymethyl group. The hydroxymethyl group at the nonreducing end shows 12 transitions between all three staggered rotamers. There is only one transition into the *tg* conformation that is stable for 20 ps. The population ratio $gg : gt : tg = 80 : 20 : 0$ at the reducing glucose and $gg : gt : tg = 40 : 55 : 5$ at the nonreducing glucose appears only slightly affected by the additional gauche potential. The average values of $\omega_{gg} \approx -56°$, $\omega_{gt} \approx 53°$, and $\omega_{tg} \approx 165°$ are shifted by about 10° with respect to the MD simulations (run wb1) without the additional gauche potential (Table III). The hydroxyl dihedral angles and occurrence and life-

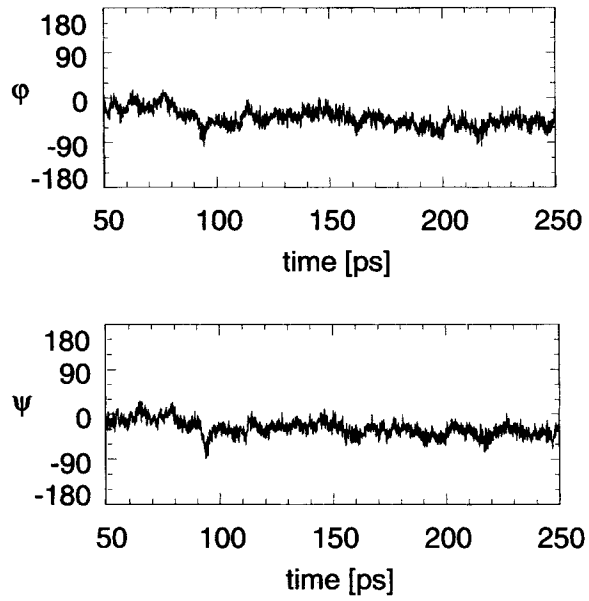

FIGURE 3. Trajectory of the φ and the ψ angle during 200-ps free MD simulation wb1.

times of hydrogen bonds closely resemble those observed in run wb1. The total energy decreases by 13 kJ mol^{-1} during this run, which is completely accounted for by the decrease in the solvent–solvent interactions.

MD Simulation in Water at 350 K, Run w35

The first calculation for maltose at a higher temperature was carried out in an isotropically scaled water box containing 137 water molecules. During the equilibrium phase, the glycosidic linkage occupied the region of the global minimum with average $\varphi = -44°$, a standard deviation of 19°, and $\psi = -34° \pm 18°$. The φ angle ranged from $-97°$ to 15° and the ψ angle varied between $-111°$ and 31° (Fig. 4). No transitions of the glycosidic linkage into other minima were found during the MD simulation. The hydroxymethyl group of the reducing residue occupies the *gt* conformation with $\omega = 67° \pm 18°$ for 80% of the time. The *tg* conformation is accessed six times for very short periods of time. The maximal lifetime of a *tg* conformer was $\approx$ 10 ps. The *gg* conformer was accessed once for $\approx$ 4 ps. The hydroxymethyl group of the nonreducing residue stays almost all the time in the *gg* conformation that has an ω angle of $-65° \pm 16°$, and changes only once for 4 ps into a *gt* conformer (Table III).

MD Simulation in Water at 400 K, Run w40

Similar to MD run w35, the trajectories of the energy components were stable throughout the calculation. The average values of the glycosidic linkage dihedral angles are $\varphi = -48° \pm 17°$ and $\psi = -38° \pm 18°$. The range of the φ-angle values is from $-110°$ to 15° and that of the ψ-angle values if from $-116°$ to 37° (Fig. 4). The hydroxymethyl group at the reducing end is found in the *gg* conformation between about 70 and 160 ps. During the other 110 ps, 18 transitions between the *gt* and the *tg* conformers occurred, giving rise to a population distribution of $gg : gt : tg = 48 : 34 : 18$. The hydroxymethyl group at the nonreducing end changes more often between the *gt* and *gg* conformations resulting in a total of 17 transitions and an overall population ratio of $gg : gt : tg = 44 : 49 : 6$ (Table III). Although the hexose ring conformations were stable, the standard deviations of the internal dihedral angles were in the range between 10° and 15°, which is significantly larger than the standard deviations obtained at 300 and 350 K, which were between 8° and 10°.

Several short-lived hydrogen bonding patterns were observed. The most frequently observed hydrogen bond occurred between the two hydroxymethyl groups. In 6% of the MD simulation, the hydroxymethyl group of the reducing end acted as a hydrogen bond acceptor, and in 2% of the time it took the role of the hydrogen bond donor. The hydrogen bond between OH3 of the reducing end and OH2′ of the nonreducing residue was observed in 4% of the conformations at different times of simulation. This hydrogen bond was also the most stable at the lower temperatures; in particular at 350 K, it appeared for 9% of the time. Hydrogen bonds between the hydroxyl groups OH4′ and OH6′ are observed in $\approx$ 2% of the conformers.

MD Simulation in Water at 600 K, Run w60

Since the MD simulation with a temperature parameter of 400 K showed no transitions out of the global minimum of the glycosidic linkage within 200-ps simulation time, the temperature parameter was raised to 600 K and a 950-ps MD trajectory was calculated. The accessible configuration space of the glycosidic linkage drastically increased (Fig. 4). The glycosidic linkage adopts one major conformation in the region of the global minimum at $\varphi/\psi \approx -60°/-45°$. A second local

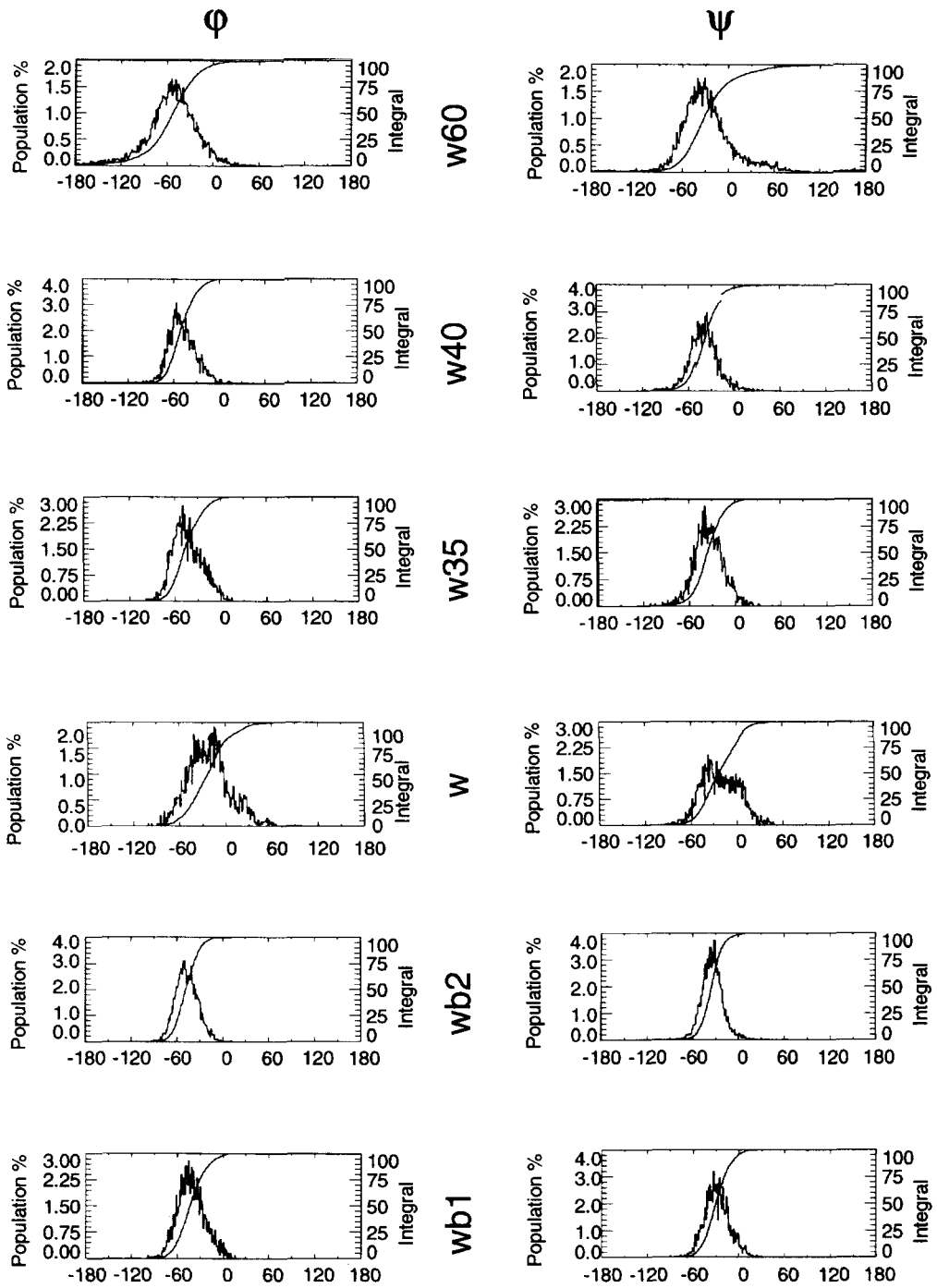

FIGURE 4. Population plots and corresponding integrals for the φ (left) and the ψ angles (right) of the MD simulation (from bottom to top) runs wb1, wb2, w, w35, w40, and w60. *Note:* the scaling of the "Population" axis differs between the different figures.

minimum with $\varphi/\psi \approx -25°/170°$ is populated for only 1% of the time. A high number of transitions are observed for the ω angles that reached all rotamers. Additionally, a total of 13 transitions between the $^4C_1$ and $^1C_4$ hexose ring conformers were observed, giving rise to 45:55% of $^4C_1$:$^1C_4$ conformations for both pyranoses. These equilibria do not agree with experimentally determined values. However, the data allow for an analysis of the influence of the pyranose ring conformation on the

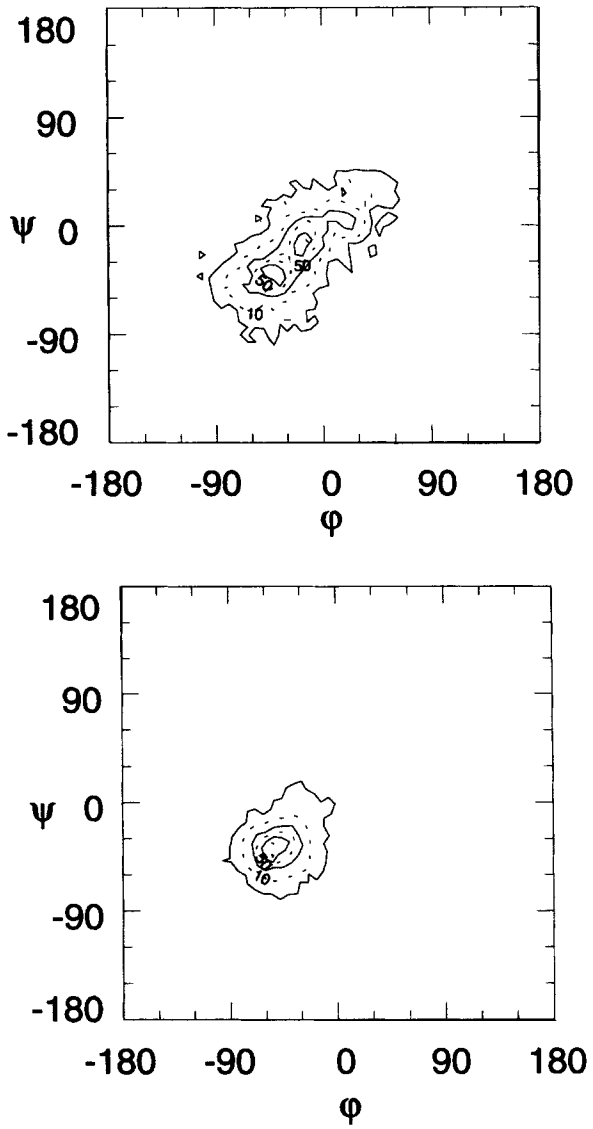

FIGURE 5. Contour plot of the populations in φ/ψ space obtained from MD simulation w (top) and run wb2 (bottom). The conformations are pooled into 6° bins and the contours are shown relative to the bin with the highest population normalized to 100%. The contour lines represent populations (outside to inside) of 1, 10 (dashed line), 30, 50 (dashed line), 70, and 90% (dashed line) relative to that of the highest populated bin.

glycosidic linkage. Using cluster analysis, it was found (data available as supplementary material) that certain areas of the conformational space are more easily accessible if the reducing or the nonreducing ring are in a $^1C_4$ conformation. The conformations were distributed into 19 clusters according to ring conformations and glycosidic linkage conformation.

MD Simulation in Water without Exo-Anomeric Potential, Run w

The potential energy parameters published by Koehler et al.[24] were used in this 250-ps MD simulation without the additional potential to account for the exo-anomeric effect. The energy minimized start conformation and the solvent box containing 137 water molecules were the same as those used in the simulations at higher temperatures described above. The energy of the ensemble was stable over the whole run.

The conformation of the glycosidic linkage shows a high degree of flexibility. The ranges of the φ and ψ dihedral angles extend over $\approx 160°$, i.e., from $-100°$ to 66° and from $-108°$ to 48° for φ and ψ, respectively (Fig. 5). About 25% of the conformations have positive φ/ψ angles. Results from a more detailed analysis of the different conformations with respect to φ, ψ, and ω using cluster analysis is included in the supplement. The lack of the exo-anomeric potential at the reducing end is apparent in the $\approx 20\%$ decreased population of the hydroxyl group OH1 in a minimum centered around a dihedral angle φ of $\approx -80°$. This hydroxyl group has a second minimum with 35% population with the hydroxyl hydrogen trans to O5. A strong increase in the stability of hydrogen bonding in particular between OH3 and O2′ is connected to the increase of positive φ/ψ angles for the glycosidic linkage. In fact, the C3—O3 dihedral is positively correlated to φ and ψ with correlation coefficients of 0.3 and 0.4, respectively. The HO3—O2′ hydrogen bond is observed 30% of the time, while it is present for only about 5% when the exo-anomeric potential reduces the population of conformers with positive φ/ψ angles.

MD SIMULATION *in vacuo*

Three 500-ps *in vacuo* MD simulations were run to evaluate the influence of the newly defined exo-anomeric potential and to compare these calculations with the MD simulations of maltose in water. One MD calculation was carried out using the force field of Koehler et al.[24] Two additional MD calculations, run vb and vc, were run with the addition of the exo-anomeric potential energy term and bond length and angle parameters for the glycosidic linkage. In the MD simulation vc, the exo-anomeric effect was also introduced to the reducing hydroxyl group. In all simulations *in vacuo*, strong intramolecular hydrogen bonds were observed that restrict the rotational freedom of

hydroxy and hydroxymethyl groups and led to artificial correlations between exo-cyclic dihedral angles.

MD Simulation In Vacuo without Exo-Anomeric Potential Energy Term, Run va

The conformation of the glycosidic linkage during the 500-ps MD simulation is characterized by average values of $\varphi/\psi = -18°/-16°$ with standard deviations of 12° and 18°, respectively. The accessed range of the φ angle is between $-54°$ and 27° and the ψ angle adopts values between $-75°$ and 55°. The conformation of the glycosidic linkage remains within this energy minimum (Fig. 6a). The hydroxymethyl group of the reducing residue is in a *gg* conformation throughout the simulation. The hydroxymethyl group of the nonreducing residue has 17 transitions between all three staggered conformers that are nearly equally populated (Table III).

The hydroxyl group of the reducing end, OH1, is trans to O5 for 75% of the time. More than 140 transitions into conformers that follow the exo-anomeric effect are observed. All other hydroxyl groups populate a single rotamer or have only a few transitions into other short-lived conformers. The major conformations have the hydrogen of the hydroxyl groups pointing toward the oxygen atoms with the higher sequence numbers (i.e., HO2 points to O3).

MD Simulation of Maltose In Vacuo with Exo-Anomeric Potential, Run vb

During this MD run the dihedral angles of the glycosidic linkage occupied a single minimum with $\varphi = -20°$ and $\psi = -17°$ only slightly affected by the additional potential. The standard deviations are 13° for both dihedral angles, and the range accessed during the 500 ps of the simulation is between $-103°$ and 33° for φ and between $-77°$ and 33° for ψ.

The hydroxymethyl group of the nonreducing end has 20 transitions between the three staggered conformers. The *tg* conformer is populated for 75% of the time. The *gt* conformer is accessed six times resulting in a population of 15%. In the reducing residue, the population ratio of the three staggered conformers is *gg* : *gt* : *tg* = 70 : 20 : 10 (Table III). The interresidue hydrogen bond with OH3 as donor and OH2′ as acceptor is found in 88% of the conformations. The hydrogen bond between both primary hydroxyl groups from OH6′ to O6 is stable if the nonreducing residue adopts a *gt* conformation.

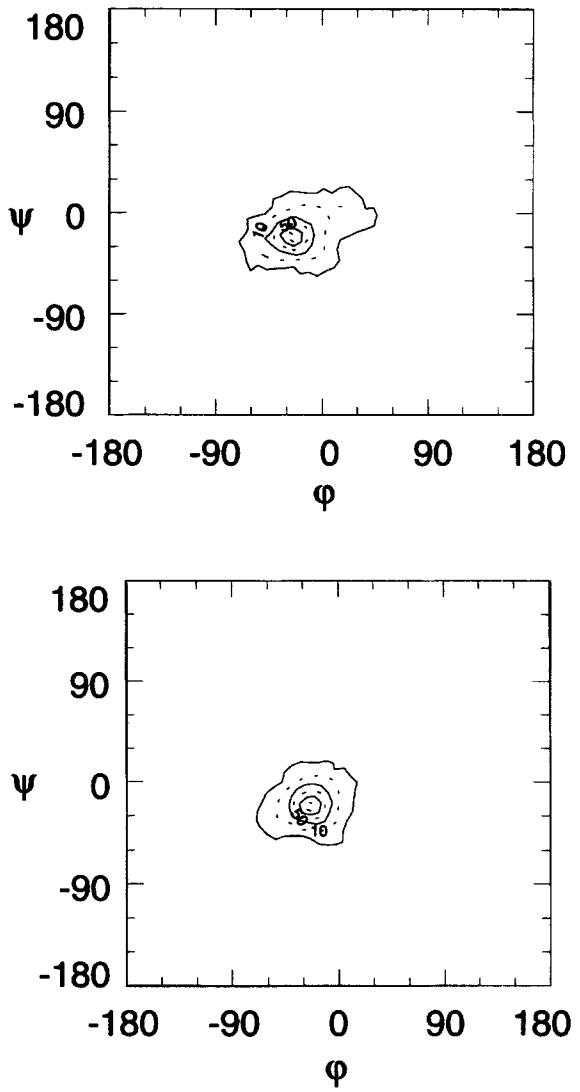

FIGURE 6. Comparison of the accessible conformational space of the glycosidic linkage *in vacuo* using different force field modifications. The population of the φ and ψ angles are displayed in a contour representation (see Fig. 5 for details). (Top) Contour plot calculated from run va (no exo-anomeric potential); (bottom) from run vc (with exo-anomeric potential). Run vb yields essentially the same contour map as run vc.

MD Simulation of Maltose In Vacuo with Exo-Anomeric Potential, Run vc

In the third calculation *in vacuo*, the same start conformation and force field parameters were used except that the exo-anomeric effect for the reduc-

ing hydroxyl group was introduced. This MD simulation (Fig. 6b) resulted in an almost identical conformational space occupied by the glycosidic linkage as in run vb, but only the hydroxymethyl group of the reducing end stays in the *gg* conformer for the complete simulation time. The ω angle of the nonreducing end has eight transitions between the *tg* conformer that is populated for 75% of the time and the *gt* conformer that accounts for the remaining 25% of the simulation time (Table III).

Discussion

EXO-ANOMERIC EFFECT

The parametrization of the exo-anomeric effects for the α and the β anomers of *O*-linked oligosaccharides was achieved by fitting the difference between the adiabatic potential energy function of the φ dihedral angle to values obtained from STO/6-31G* *ab initio* calculations.[42] For the β anomer, the resulting empirical energy function gave a nearly perfect fit with the data obtained from *ab initio* calculations, while the corresponding curve for the α anomer initially showed differences between the force field derived energy values and the energy values from the *ab initio* study. With two additional energy values from STO/6-31G* *ab initio* calculations at $\varphi = -30°$ and $-90°$ (ref. 43) and a fitting procedure that gave less weight to the high energy conformations, especially at $\varphi \approx -120°$, it was possible to describe the conformational energies of the α conformer with reasonable accuracy. Comparing the energy functions of the *ab initio* and the updated force field, it is clear that the new force field parametrization slightly underestimates the energy of conformations with φ angles of less than $-60°$. With different weight factors for the fit, a better overall agreement between empirical and *ab initio* data could be achieved. It would reduce the accuracy in the representation of the energy minima regions or introduce additional minima at $\varphi = 150°$. Alternatively, the fit for the potential between $\varphi = -60°$ and $-30°$ could be improved with more parameters in the fit and more *ab initio* data. However, it is important to note that the agreement between the energy curves should not be overestimated. All these model calculations, empirical force field and *ab initio*, are performed *in vacuo* and the interactions of the atoms responsible for the exo-anomeric effect with water molecules are likely to influence the shape of the energy surface. Such a reduction of the energy contribution of the anomeric and exo-anomeric effect has been discussed by Praly and Lemieux.[51] It is expected to introduce changes of 1–2 kcal mol^{-1} into the corresponding energy curve. In addition, a very accurate description of a single parameter would only be of value if other important parameters of the force field are of similar accuracy (see below). The deviation between the current parametrization and the *ab initio* data might introduce small errors into the energy maps of carbohydrates, i.e., a slightly higher population of conformations with φ angles of about $-90°$ for α-D-maltose. However, these conformers are not populated *in vacuo* (cf. run va, vb, and vc) because of hydrogen bonds stabilizing the other conformers. They are found in MD simulations in water (see below). In fact, as shown in a forthcoming study,[37] higher populations of these conformations are supported by optical rotation data which agree excellently with time average values for the molar rotation calculated from the MD population distribution.

For α-D-maltose, the introduction of the exo-anomeric effect reduced the probability of conformations with high φ/ψ dihedral angles (Figs. 5, 6). The population distribution of the MD simulation w (without the exo-anomeric potential) has considerable higher population at positive φ/ψ angles than the MD runs wb1, wb2, and other MD simulations at 300 K.[37] About 20% of the population in run w is characterized by positive φ/ψ angles. In all other calculations, even at increased temperature, these conformations are only rarely populated. The comparison of the simulations *in vacuo* with (runs vb and vc) and without (run va) the exo-anomeric effect for the *O* glycosidic linkage resulted in similar conclusions as drawn from the simulations in water. The differences between the *in vacuo* simulations are smaller because of the strong influence of the hydrogen bonds that reduces the relative weight of the exo-anomeric potential.

The separate parametrization of the exo-anomeric effect of the reducing hydroxyl group OH1 became necessary since the strong electrostatic interactions between the HO1 and the O5 and the lack of a van der Waals radius for HO1 resulted in a too strong attraction between these atoms, as is evident from a comparison of the potential energy function for a rotation around the C1—O1 bond between *ab initio* studies on methoxymethanol[41] and the GROMOS force field. This also causes problems during energy mini-

mization and during the first MD steps when the molecule has a fairly high potential energy. In such a situation, the light hydroxyl proton may come close to the O5 ring oxygen leading to a deformation in the bond angles and bond length of the O5—C1—O1—HO1 unit from which it is difficult to recover. Although this artifact could be avoided by choosing very small step sizes for the energy minimization algorithm or the integration step in the MD simulation, the current parametrization with the HO1—O5 interaction described exclusively by a dihedral potential avoids these problems altogether and better describes the potential of the φ rotation of the reducing hydroxyl group.#

It has been emphasized that a change of or an addition to the parameters of an existing force field has to preserve the balance of the force field.[7] The parametrization described here changes only interactions within the O5—C1—O1—Cx/HO1 units. Nonbonded interactions between these atoms and other atoms were not modified. The equilibrium values of the O5—C1 and O1—C1 bond length and the O5—C1—O1 bond angle were adjusted with respect to the existing van der Waals and electrostatic interactions. The corresponding force constants were chosen to be consistent with the GROMOS classification scheme.[24]

SOLVENT EFFECTS ON MALTOSE CONFORMATION

In simulations *in vacuo*, the average conformations of the glycosidic linkage have smaller φ and ψ angles compared with simulations in water. The change in the linkage conformation from $\varphi/\psi \approx -20°/-17°$ *in vacuo* to $-40°/-31°$ in water is mainly caused by interresidue hydrogen bonds that are formed between the OH3 and the OH2' that restrict the accessible conformational space to φ/ψ angles of less than about 30°. While this hydrogen bond is only transiently found in the MD simulations in water, it is found in over 80% of the conformations of the *in vacuo* MD runs. In water there is no net gain in enthalpy due to the formation of this hydrogen bond since hydrogen bonds with water can be formed instead. In addition, the rotameric distribution of the hydroxymethyl groups, in particular that of the reducing end, is strongly distorted due to intramolecular hydrogen bonds. The population distribution found *in vacuo* is not in agreement with experimental results for maltose in water. In contrast, the population distribution found in the simulations in water is well confirmed by experimental findings.[37]

The nonbonded HO1—O5 interactions are removed from the force field by adding the O5 atom to the exclusion list for 1-3 pairs of HO1. This ensures that no other interactions are affected.

INFLUENCE OF SIZE OF WATER BOXES

The drop in the electrostatic interaction energy between the solvent molecules that was observed between the first 250 ps of run wb (run wb1) and the remaining 500 ps (run wb2) can be attributed to the equilibration of the water box indicating that several hundred picoseconds might be necessary to equilibrate a large water box.[37] It was also found that the water box with 137 water molecules that was used for the high temperature calculations was not in equilibrium at 300 K, and attempts to equilibrate this ensemble without restraints caused ring inversions and other high energy conformations of the solute to occur. In contrast, a solvent box containing 160 water molecules[37] was found to be large enough for the simulation of maltose at 300 K. One of the reasons that the initial choice of the water box settings is critical is that an isotropic scaling of the box size was used to avoid a solute and its "periodic boundary image" coming too close to each other.

INFLUENCE OF SIMULATION TEMPERATURE

The increased mobility of the glycosidic linkage in MD simulations at 350 and 400 K resulted only in a slightly increased sampling efficiency of its conformational space. The local energy minimum region was not left and a slight underrepresentation of smaller φ and ψ angles is evident even at 400 K as compared to 5.4-ns MD simulations[37] at 300 K. The average lifetime of the hydroxymethyl group of the nonreducing glucose in the *gg* and the *gt* conformation is about 25 ps at 400 K, that is, as expected, much lower than the average lifetime of 200 ps observed at 300 K.[37] However, neither the reducing glucose's hydroxymethyl group nor the glycosidic linkage dihedral angles are in an equilibrium state at that point.

Increasing the temperature parameter to 600 K, the high kinetic energy increased the flexibility of the glycosidic linkage so that conformational transitions were observed. In part, this increase was caused by interconversions between the conformations of the pyranose rings that adopted both the $^4C_1$ and the $^1C_4$ conformations. The subset of con-

formations that had both hexoses in the $^4C_1$ conformation revealed a less strong increase in the flexibility of the glycosidic linkage. A second local minimum in the φ/ψ space that is characterized by a ψ angle of about 180° was accessed for a short time. It was accessed via a low energy saddle between $\psi \approx 120°$ and 160°. This minimum was further investigated in MD simulations at 300 K.[37] The high population of the $^1C_4$ conformers is not in agreement with the experimentally derived energy difference between the $^1C_4$ and the $^4C_1$ conformation. This indicates that the parametrization of the force field is not suitable for calculations at temperatures of 600 K or more.

GAUCHE POTENTIAL

The gauche effect describes a stereoelectronic interaction that influences the conformational preferences in the O—C—C—O fragments of oligosaccharides.[50] In the simulation at 600 K as well as in some of our preliminary test simulations at 300 K that were not in equilibrium (data not shown), we found ring inversions from the $^4C_1$ into the $^1C_4$ conformation. Modeling studies *in vacuo* revealed that in the GROMOS force field the $^4C_1$ conformation of a glucose is more stable by about 20 kJ mol^{-1}, which is expected from experimental evidence. However, in simulations with explicit introduction of water, local minima of the solvent conformation can be found that stabilize the $^1C_4$ conformation. In addition, in the $^1C_4$ conformation of the pyranose ring, the bond angles are widened by some degree such that the unfavored nonbonded 1–3 interactions between O2 and O4 of glucose are reduced. Together with stabilization due to carbohydrate–water interactions, this can drastically lower the energy of the $^1C_4$ conformation. A study of individual interactions between all atoms within a glycosyl residue indicated this phenomenon might be caused by an imbalance in the existing force field, in particular an imbalance between bond angle potentials and interactions for 1–3 diaxial pairs and between dihedral potentials and charge interactions in O—C—C—O units. A parametrization based on *ab initio* studies of model compounds such as ethylene glycol[52] and 1,2-dimethoxyethane[52,53] yielded results that do not explain the experimental observed gauche effect,[50] indicating that the high complexity of a solvated carbohydrate precludes a complete theoretical description *in vacuo* and, thus, a parametrization similar to that performed for the exo-anomeric effect.

We investigated the use of an additional dihedral potential that reduced the energy of all O—C—C—O units, the secondary alcohol groups as well as the hydroxymethyl groups, in the gauche orientation by about 4.5 kJ mol^{-1}. This empirically derived modification of the force field resulted in a slight decrease of the mobility of the hexose ring indicated by a 1° reduced standard deviation but hardly affected the conformation of the hexose rings. In contrast, the average dihedral angles of the hydroxymethyl groups changed by about 10° compared with the simulation without the gauche potential. The simulation was too short to reach an equilibrium for the hydroxymethyl rotations. Currently, there are not enough experimental data to distinguish between the differences in populations of 5–10% or the average dihedral angle of 10° in the staggered rotamers of the hydroxymethyl groups.

From the simulations and our model studies, we conclude that a better description of the gauche interaction would need more than the addition of a dihedral potential. It would be probably necessary to adjust the bond angle terms together with the 1–4 charge and van der Waals interaction. These parametrizations would require including the solvent effects explicitly. The computational effort to achieve this would be tremendous. Fortunately, the current parametrization works well enough at moderate temperatures and as long as the system is in thermal equilibrium, such that we do not see a strong necessity for adjusting these parameters at present. The additional gauche potential should be considered for equilibration phases or high temperature simulations.

Conclusion

The MD simulations *in vacuo* not only result in conformations that are in poor agreement with experimental findings, they also incorrectly describe the dynamical behavior of the oligosaccharide. In contrast, NMR and optical rotation studies[54–58] of α-D-maltose and methylmaltoside are in good agreement[37] with glycosidic linkage conformations that have φ/ψ dihedral angles of about $-50°/-40°$ as derived from long MD simulations in water with the modified GROMOS force field. Similarly, the low population of *tg* conformers for the hydroxymethyl groups found in water agrees with experimentally derived NMR coupling constants.[58] We conclude that the solvent has a major

impact on the conformational preferences of maltose and should be included in simulations of oligosaccharides. Furthermore, force field studies that incorporate relatively high charges on atoms or strong hydrogen bond terms cannot correctly represent the conformational behavior of molecules without compensation.

MD simulations, even when extending to several hundred picoseconds, are too short to represent ensemble averages of flexible molecules like oligosaccharides. Their relative mobile hydroxymethyl groups have lifetimes that are in the range or extending these simulation times. Moreover, transitions of the glycosidic linkage dihedral angles cannot be expected to occur within subnanosecond MD simulations. Summarizing the experiences with the calculations in different environments, we found that at moderately raised temperature, the transition probability between different conformational states can be increased. At much higher temperature than room temperature, the force field shows an imbalance that leads to conformations that are of minor interest. To achieve an unbiased estimate of the ensemble averaged conformational properties as well as to analyze conformational freedom, we propose longer MD simulations extending to several nanoseconds of simulation time. Such an approach is presented in a forthcoming study.[37]**

Acknowledgment

This work was supported in part by a grant to Dr. Ott from the scientific committee of NATO via the DAAD.

References

1. W. F. van Gunsteren and H. J. C. Berendsen, *Angew. Chem. Int. Ed. Engl.*, **29**, 992 (1990).
2. S. W. Homans and M. Forster, *Glycobiology*, **2**, 143 (1992).
3. W. F. van Gunsteren, *Curr. Opin. Struc. Biol.*, **3**, 277 (1993).
4. J. P. Carver, D. Mandel, S. W. Michnick, A. Imberty, and J. W. Brady, *ACS Symp. Ser.*, **430**, 266 (1990).
5. A. T. Brünger and M. Karplus, *Acc. Chem.*, **24**, 54 (1991).
6. R. Brüschweiler, B. Roux, M. Blackledge, C. Griesinger, M. Karplus, and R. R. Ernst, *J. Am. Chem. Soc.*, **114**, 2289 (1992).

**A supplement is available containing a table of the average energy values for all runs and the description and results of the cluster analysis for runs w and w60 (see footnote * on page 1068). Residue topologies files for a variety of sugar residues and modified parameter files for GROMOS are available upon request (E-mail: ottk@pt.cyanamid.com).

7. W. F. van Gunsteren and A. E. Mark, *Eur. J. Biochem.*, **204**, 947 (1992).
8. B. Meyer, *Topics Curr. Chem.*, **154**, 141 (1990).
9. I. Tvaroska, S. Pérez, O. Noble, and F.-R. Taravel, *Biopolymers*, **26**, 1499 (1987).
10. J. E. H. Koehler, W. Saenger, and W. F. van Gunsteren, *Eur. Biophys. J.*, **16**, 153 (1988).
11. J. E. H. Koehler, W. Saenger, and W. F. van Gunsteren, *J. Biomol. Struct. Dynamics*, **6**, 181 (1988).
12. J. E. H. Koehler, W. Saenger, and W. F. van Gunsteren, *J. Mol. Biol.*, **203**, 241 (1988).
13. L. M. J. Kroon-Batenburg and J. Kroon, *Biopolymers*, **29**, 1243 (1990).
14. B. P. van Eijck, L. M. J. Kroon-Batenburg, and J. Kroon, *J. Mol. Struct.*, **237**, 315 (1990).
15. H. Beierbeck and R. U. Lemieux, *Can. J.*, **68**, 820 (1990).
16. Z. Y. Yan and C. A. Bush, *Biopolymers*, **29**, 799 (1990).
17. S. Ha, J. Gao, B. Tidor, J. W. Brady, and M. Karplus, *J. Am. Chem. Soc.*, **113**, 1553 (1991).
18. B. J. Hardy and A. Sarko, *J. Comput. Chem.*, **14**, 848 (1993).
19. J. W. Brady and R. K. Schmidt, *J. Phys. Chem.*, **97**, 958 (1993).
20. S. N. Ha, A. Giammona, M. Field, and J. W. Brady, *Carbohydr. Res.*, **180**, 207 (1988).
21. S. W. Homans, *Biochemistry*, **29**, 9110 (1990).
22. N. R. Krishna, B.-Y. Choe, M. Prabhakaran, G. C. Ekborg, L. Rodén, and S. C. Harvey, *J. Biol. Chem.*, **265**, 18256 (1990).
23. Z.-Y. Yan, B. N. N. Rao, and C. A. Bush, *J. Am. Chem. Soc.*, **109**, 7663 (1987).
24. J. E. H. Koehler, W. Saenger, and W. F. van Gunsteren, *Eur. Biophys. J.*, **15**, 97 (1987).
25. J. E. H. Koehler, W. Saenger, and W. F. van Gunsteren, *Eur. Biophys. J.*, **25**, 211 (1987).
26. C. J. Edge, U. C. Singh, R. Bazzo, G. L. Taylor, R. A. Dwek, and T. W. Rademacher, *Biochemistry*, **29**, 1971 (1990).
27. J. W. Brady, *J. Am. Chem. Soc.*, **111**, 5155 (1989).
28. J. W. Brady, *Curr. Opin. Struct. Biol.*, **1**, 711 (1991).
29. S. W. Homans, *Biochemistry*, **29**, 9110 (1990).
30. M. Prabhakaran, *Biochem. Biophys. Res. Commun.*, **178**, 192 (1991).
31. G. A. Jeffrey, *J. Mol. Struct.*, **237**, 75 (1990).
32. W. F. van Gunsteren and H. J. C. Berendsen, *Groningen Molecular Simulation (GROMOS) Library Manual*, BIOMOS, Nijenbourgh 16, Groningen, The Netherlands, 1987.
33. A. E. Mark, H. J. C. Berendsen, and W. F. van Gunsteren, *Biochemistry*, **30**, 10866 (1991).
34. R. M. Sok, H. J. C. Berendsen, and W. F. van Gunsteren, *J. Chem. Phys.*, **96**, 4699 (1992).
35. W. F. van Gunsteren, H. J. C. Berendsen, R. G. Geurtsen, and H. J. R. Zwinderman, *Ann. NY Acad. Sci. USA*, **482**, 287 (1986).
36. H. Thogersen, R. U. Lemieux, K. Bock, and B. Meyer, *Can. J. Chem.*, **60**, 44 (1982).
37. K.-H. Ott and B. Meyer, *MD Simulations of Maltose in Water*, *Carbohydr. Res.*, to appear.
38. Precision Visuals, Inc. Boulder, CO, 1989.
39. Tripos Associates, Inc., St. Louis, MO, 1992.

40. Digital Equipment Co., *Users Reference*, Maynard, MA, 1991.
41. G. A. Jeffrey, J. A. Pople, and L. Radom, *Carbohydr. Res.*, **38**, 81 (1974).
42. K. B. Wiberg and M. A. Murcko, *J. Am. Chem. Soc.*, **111**, 4821 (1989).
43. B. Meyer, Unpublished data, 1990.
44. Linde D. R., Ed., *CRC Handbook of Chemistry and Physics*, 73rd ed., CRC Press, Boca Raton, FL, 1992–1993, p. 9-7, 9-8.
45. W. F. van Gunsteren and H. J. C. Berendsen, *Mol. Phys.*, **34**, 1311 (1977).
46. Lotus 123, Lotus Development Co., Cambridge, MA, release 3.1.
47. SigmaPlot for DOS, Jandel Scientific, San Rafael, CA, 1992.
48. H. J. C. Berendsen, P. J. M. Postma, W. F. van Gunsteren, and J. Hermans, In *Intermolecular Forces*, B. Pullman, Ed., Reidel, Dordrecht, The Netherlands, 1981, p. 331.
49. H. J. C. Berendsen, P. J. M. Postma, W. F. van Gunsteren, A. di Nola, and J. R. Haak, *J. Chem. Phys.*, **81**, 3684 (1984).
50. N. S. Zefirov, V. V. Samoshin, O. A. Subbotin, V. I. Baranenkov, and S. Wolfe, *Tetrahedron*, **34**, 2953 (1978).
51. J.-P. Praly and R. U. Lemieux, *Can. J. Chem.*, **65**, 213 (1987).
52. M. A. Murco and R. A. DiPaola, *J. Am. Chem. Soc.*, **114**, 10010 (1992).
53. D. A. Smith, R. L. Jaffe, and D. Y. Yon, *J. Phys. Chem.*, **97**, 12752 (1993).
54. D. A. Rees and D. Thom, *J. Chem. Soc. Perkin Trans. II*, 191 (1977).
55. A. Parfondry and N. Cyr, *Carbohydr. Res.*, **59**, 299 (1977).
56. G. M. Lipkind, V. E. Verovsky, and N. K. Kochetkov, *Carbohydr. Res.*, **133**, 1 (1984).
57. S. Perez, F. Taravel, and C. Vergelati, *Nouv. J. Chim.*, **561** (1985).
58. A. S. Shashkov, G. M. Lipkind, and N. K. Kochetkov, *Carbohydr. Res.*, **147**, 175 (1986).